

Supplementary Materials

One-step hydrothermal synthesis of Fe single atom doped 1T-MoS₂ nanosheets for high-performance seawater hydrogen production

Xun Geng¹, Yitong Cao¹, Zhixuan Li¹, Mengyao Li², Chaojie Cao¹, Chenxi Yu¹, Xueze Chu¹, Long Hu², Yunlong Sun², Liang Qiao³, Xiaojiang Yu⁴, Mark B. H. Breese⁴, Jang Mee Lee¹, Danyang Wang², Dewei Chu², Jiabao Yi^{1,*}

¹Global Innovative Centre for Advanced Nanomaterials, School of Engineering, University Drive, The University of Newcastle, Callaghan NSW 2308, Australia.

²School of Material Science and Engineering, The University of New South Wales (UNSW), Sydney 2033, Australia.

³School of Physics, University of Electronic Science and Technology of China, Chengdu 610054, Sichuan, China.

⁴Singapore Synchrotron Light Source, National University of Singapore, Singapore 117603, Singapore.

***Correspondence to:** Prof. Jiabao Yi, Global Innovative Centre for Advanced Nanomaterials, School of Engineering, University Drive, The University of Newcastle, University Drive, Callaghan, NSW 2308, Australia. E-mail: Jiabao.yi@newcastle.edu.au

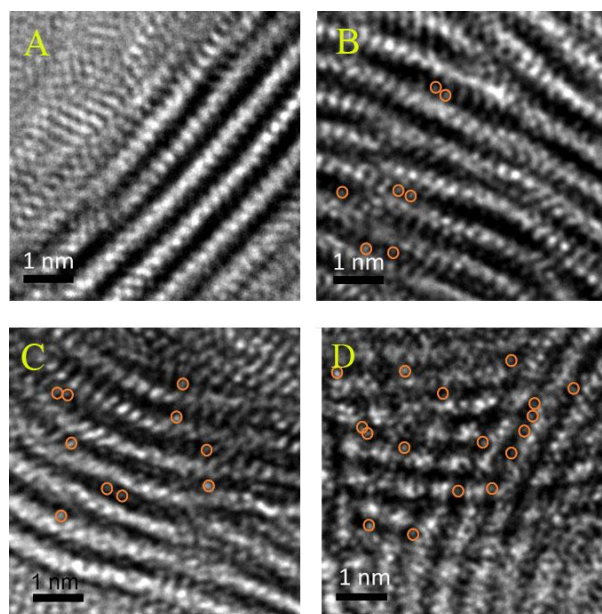


Figure 1. TEM images of (A) sample S0; (B) S2 and (C) S5 and (D) S20 respectively.

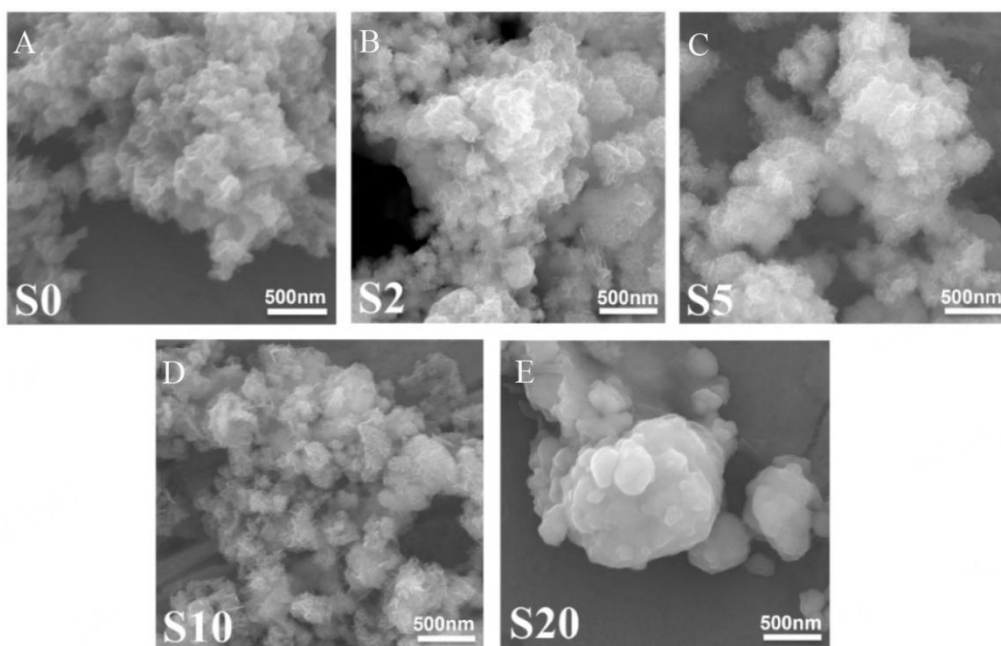


Figure 2. SEM images of sFe-1T/MoS₂ nanosheets for sample (A) S0; (B) S2; (C) S5; (D) S10 and (E) S20, respectively.

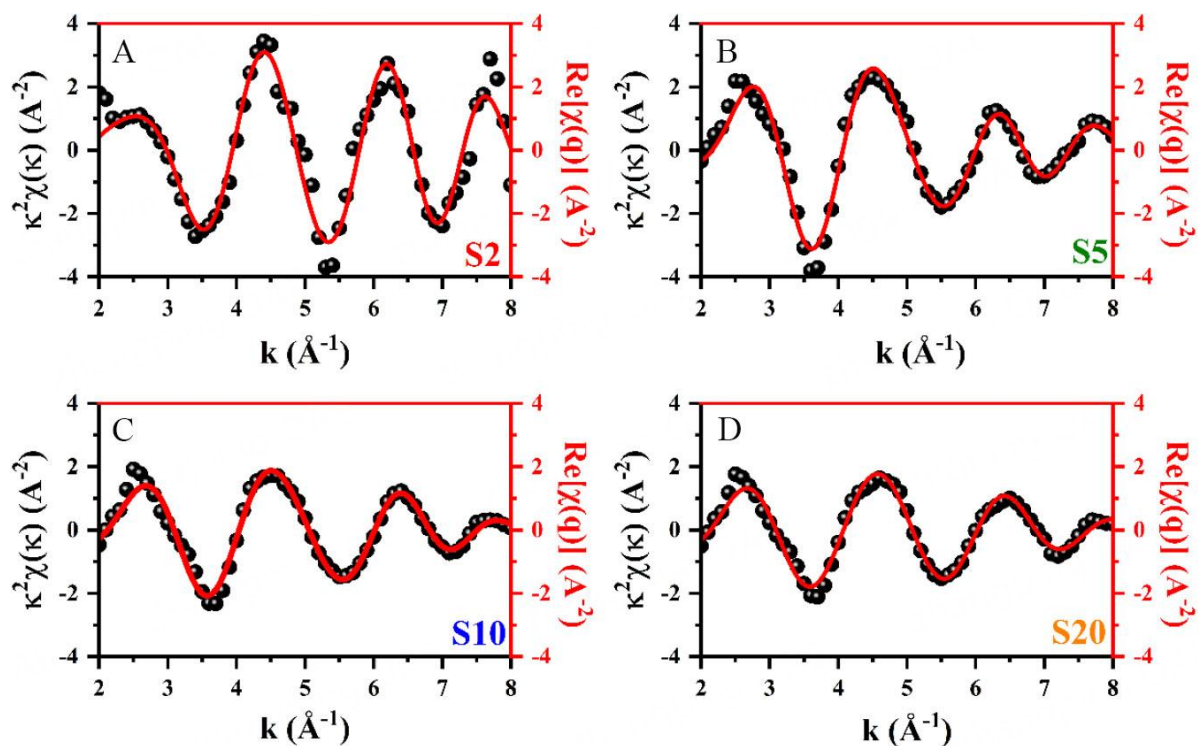


Figure 3. The forward-backward Fourier transformation (FT) transform for (A) S2; (B) S5; (C) S10 and (D) S20.

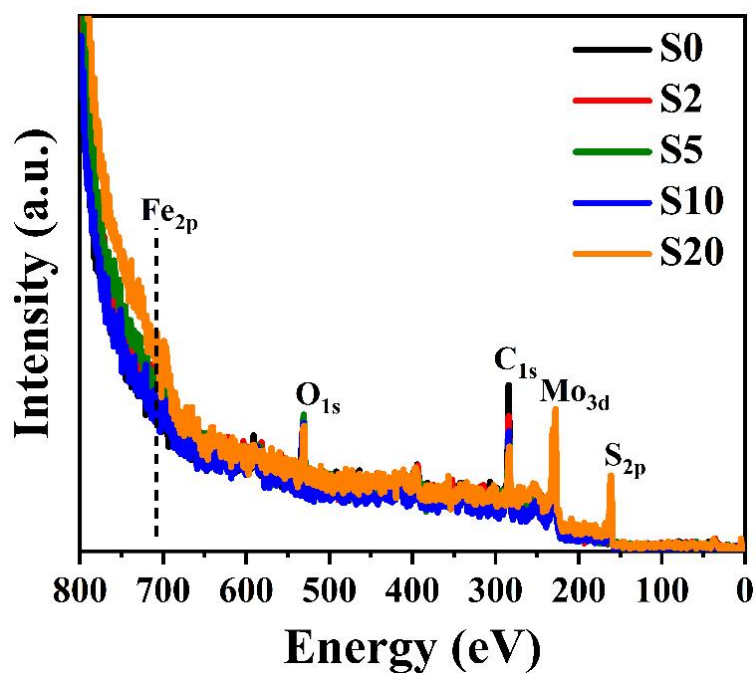


Figure 4. Survey curves of XPS for sFe-1T/MoS₂.

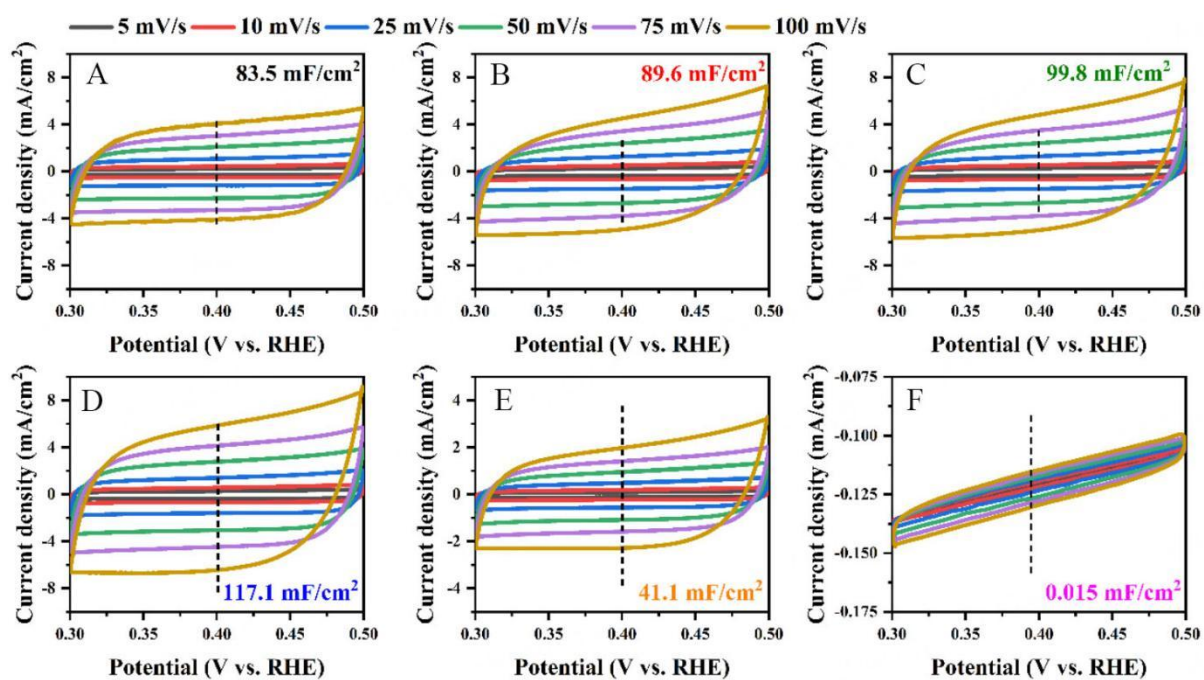


Figure 5. Non-Faradaic region Cyclic voltammetry (CV) curves at different scan rates (5, 10, 25, 50, 75 and 100 mV/s) for (A) S0; (B) S2; (C) S5; (D) S10; (E) S20 and (F) carbon electrode, respectively.

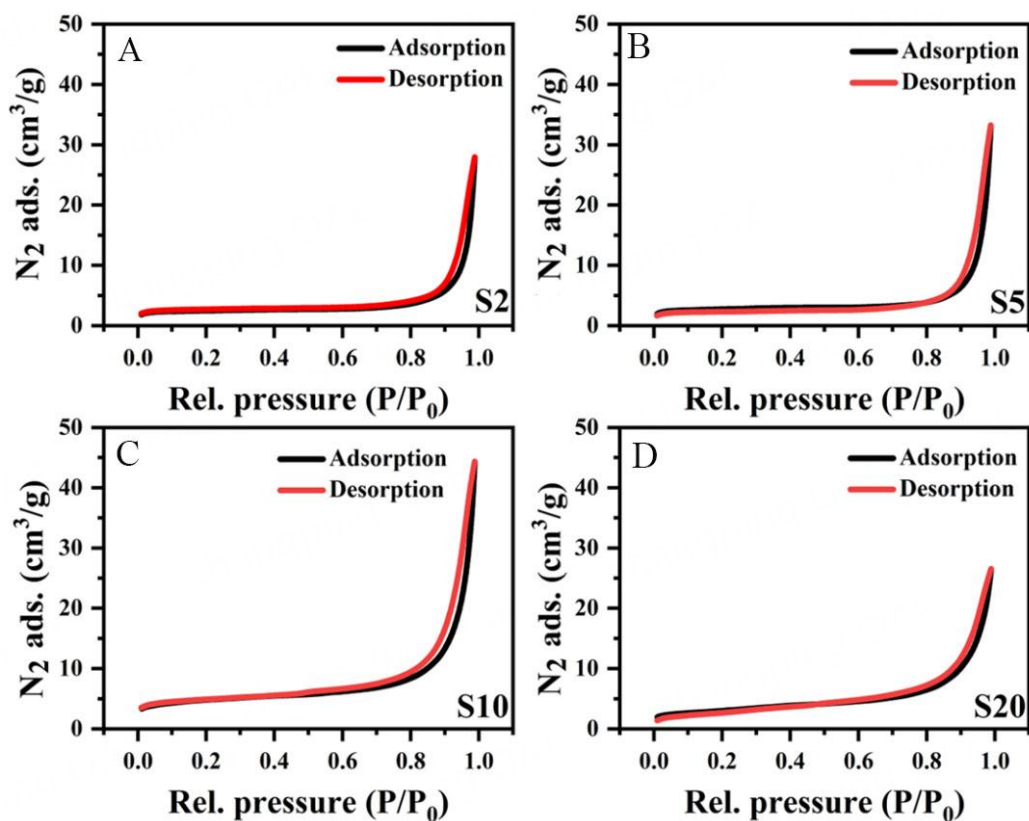


Figure 6. The N₂ absorption–desorption isotherms for sample (A) S2; (B) S5; (C) S10; (D) S20, respectively.

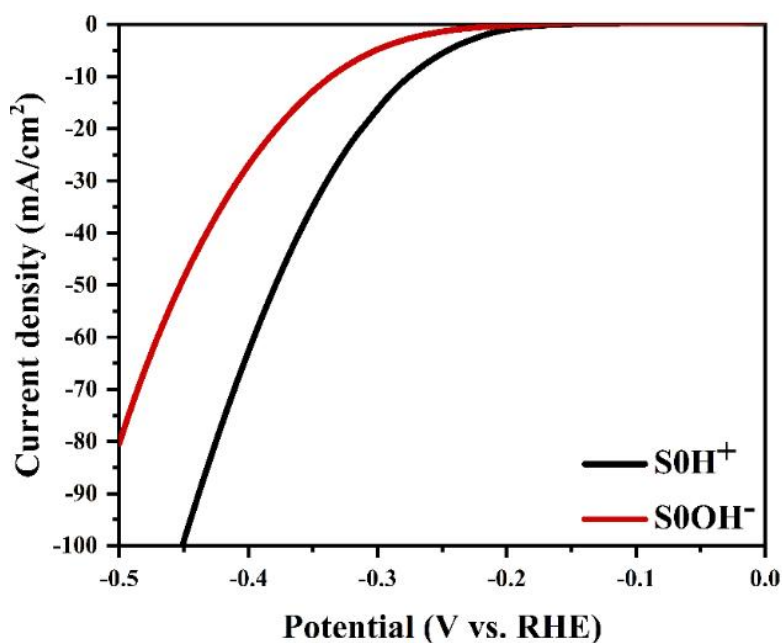


Figure 7. LSV curves of non-doped 1T MoS₂ measured in 0.5M H₂SO₄ and 1M KOH solution.

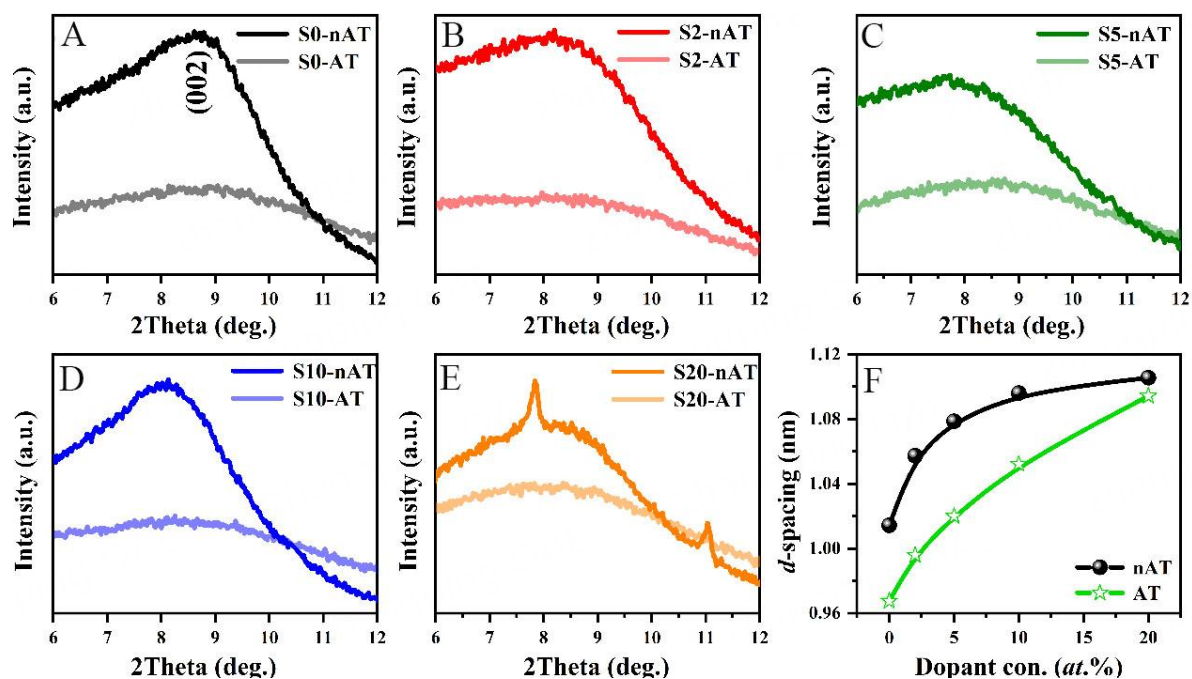


Figure 8. The zoomed-in XRD peak variation with acidic treatment (AT) and without acidic treatment (nAT) for (A) S0; (B) S2; (C) S5; (D) S10 and (E) S20; (F) The summary of *d*-spacing changes by acidic treatment.

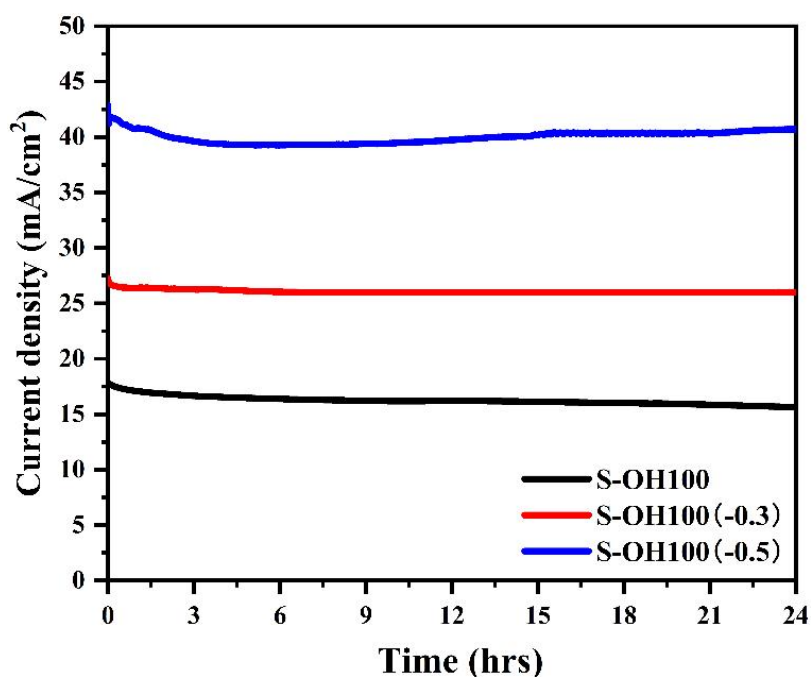


Figure 9. 24hrs stability measurement at a constant RHE potential of - 0.3 V and -0.5 V in alkaline (1M KOH) solutions, respectively.

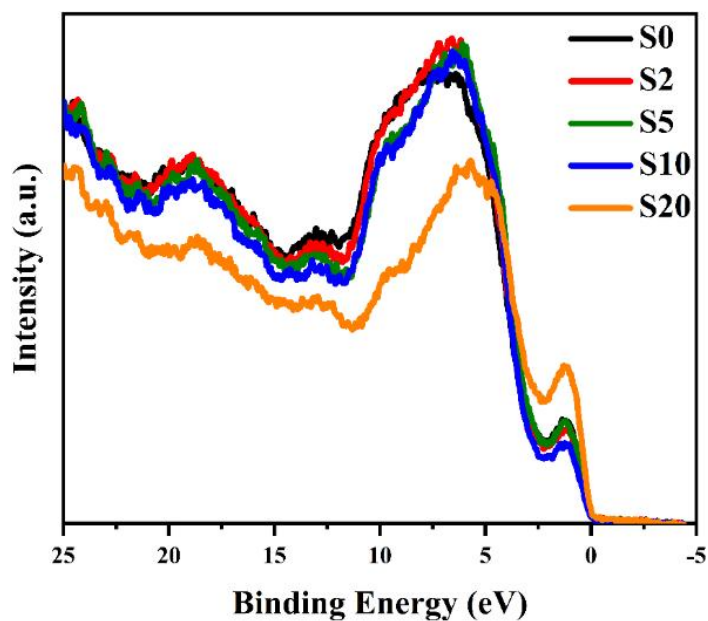


Figure. S10 Overall UPS spectra for sFe-1T/MoS₂.

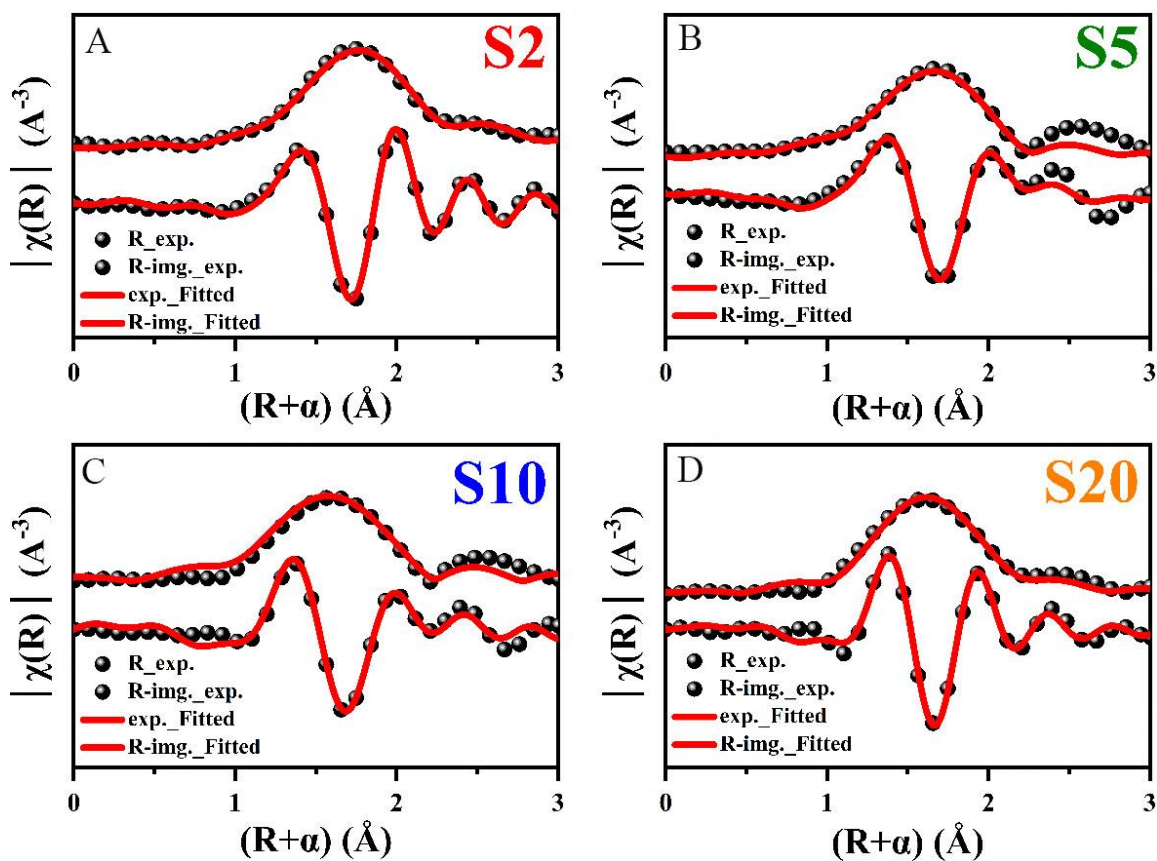


Figure 11. EXAFS Fe *K*-edge fitting curves for (A) S0; (B) S5; (C) S10 and (D) S20 for the real (R_{exp.}) and imaging (R_img.exp.) part of fitting formular, respectively.

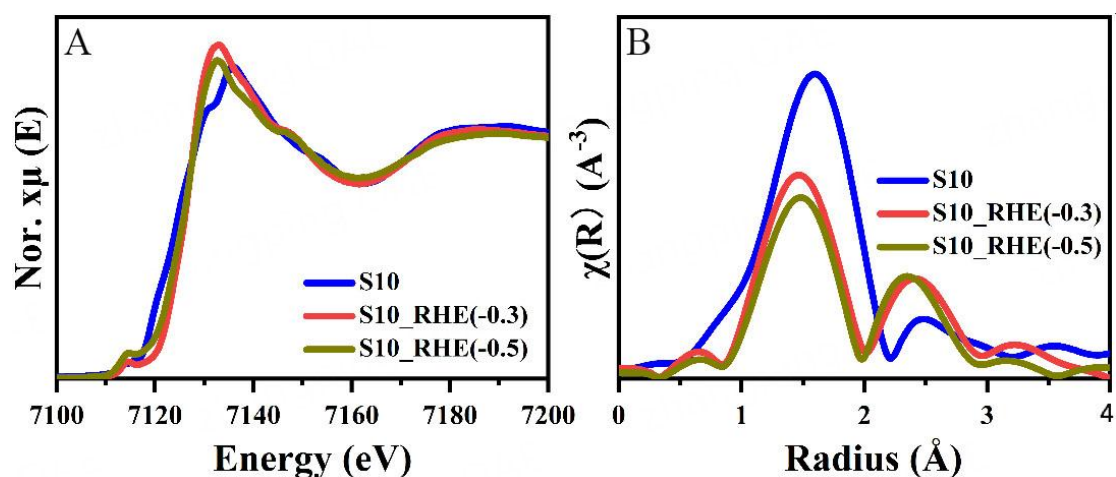


Figure 12. (A) NEXAFS curves of Fe K-edge before and after long-term catalysis at RHE potential of -0.3 V and RHE potential of -0.5 V in alkaline solution for sample S10; (B) Fourier-transform (FT) k^2 -weighted NEXAFS spectra of sample S10 before and after long-term catalysis.

Table 1. Recent milestones on single element doping of 1T/MoS₂ on hydrogen evolution reaction (HER).

Dopants	Tafel slope (mV/dec)	Loading mass (mg/cm ²)	Electrolyte	Ref.
<i>V</i>	54	0.26		[1]
<i>P</i>	67	2.8		[2]
<i>W</i>	55	0.28		[3]
<i>N</i>	93	-	0.5M H ₂ SO ₄	[4]
<i>FeS₂</i>	82	8.9		[5]
<i>Pd</i>	62	0.22		[6]
<i>Pt</i>	57	-		[7]
<i>Ni</i>	50	-	1M KOH	[8]
<i>Fe</i>	55	0.04	0.5M H ₂ SO ₄	This work

Table 2. Summary of electrochemical measurements for Fe-1T/MoS₂ in acid solution with 40 $\mu\text{g}/\text{cm}^2$ loading mass

Name	Composition	Overpotential (mV)	Tafel slope (mV/dec)	Onset potential (mV)	C_{dl} (mF/cm ²)	EASA (cm ²)
<i>S0</i>	Fe ₀ -1T/MoS ₂	274	70	245	83.3	4165

<i>S2</i>	Fe _{0.02} - 1T/Mo _{0.98} S ₂	254	57	223	89.6	4389
<i>S5</i>	Fe _{0.05} - 1T/Mo _{0.95} S ₂	234	56	210	99.8	4988
<i>S10</i>	Fe _{0.1} - 1T/Mo _{0.9} S ₂	215	55	190	117.1	5853
<i>S20</i>	Fe _{0.2} - 1T/Mo _{0.8} S ₂	260	75	230	41.4	2070

*Overpotential is obtained directly from LSV measurement at a current density of 10 mA/cm²; *Onset potential is directly obtained in Tafel plots fitting at the current density of 1 mA/cm².

Table 3. Parameters of the NEXAFS Curve fitting for the Fe *K*-edge of sFe-1T/MoS₂.

<i>Sample</i>	<i>Path</i>	<i>R_{eff}</i> (Å)	<i>N</i>	<i>R</i> (Å)	σ^2 (Å)
<i>S2</i>			6.5	2.327	0.01 ± 0.002
<i>S5</i>			6.4	2.310	0.009 ± 0.002
<i>S10</i>	Fe-S	2.239	6.1	2.293	0.006 ± 0.003
<i>S20</i>			5	2.287	0.002 ± 0.002

**R_{eff}*: the standard radius distance obtained from the standard structure of FeS; *N*: coordination number, also fixed by the standard structure of FeS; *R*: radius distance for real path; σ^2 : Debye-Waller factors are fitted based on global fit parameters. S_0^2 was fixed by 0.66, corresponding to previous reports; ΔE_0 was refined as a global fit parameter, returning a value of (-8 ± 1); Data ranges were set as from 2 to 8 for *k* and 1 to 3 for *R*, respectively; The number of variable parameters is 4. The R-factor for this fitting is 1.3%.

Table 4. Summary of seawater splitting performance of 10 at.% single-atom-doped Fe-1T/MoS₂ (S10) compared to recent Mo-based seawater electrocatalysts

Composition	Overpotential (mV) at 10mAcm⁻²	<i>Additional</i>	Ref.
<i>S-H10</i>	318	10% v/v 0.5M	This

		H ₂ SO ₄	work
<i>S-H30</i>	262	30% v/v 0.5M H ₂ SO ₄	
<i>S-OH10</i>	325	10% v/v 1M KOH	
<i>S-OH30</i>	242	30% v/v 1M KOH	
<i>CoNi-MoS₂-Pd_{SA}Ru_{SA}</i>	1450	1M KOH	[9]
<i>CC-MoC/MoS₂-H</i>	136	-	[10]
<i>CoMoP-C</i>	450	-	[11]
<i>Mo₅N₆</i>	257	pH 8.4	[12]
<i>h-MoN-BN-CNT</i>	190	-	[13]
<i>MoS₂-QDs/aerogel-100</i>	400	-	[14]
<i>Co_xMo_{2-x}C/MXene/NC</i>	312	-	[15]
<i>Fe-MoS₂ array</i>	119	-	[16]
<i>MoS₂@W-G</i>	115	1M KOH	[17]
	86	0.5M H ₂ SO ₄	

References:

1. Li M, Cai B, Tian, R, et al. Vanadium doped 1T MoS₂ nanosheets for highly efficient electrocatalytic hydrogen evolution in both acidic and alkaline solutions. *Chem Eng* 2021;409:128158.
2. Bian L, Gao W, Sun J, et al. Phosphorus-doped MoS₂ nanosheets supported on carbon cloths as efficient hydrogen-generation electrocatalysts. *ChemCatChem* 2018;10:1571-7.
3. Rong J, Ye Y, Cao J, et al. Restructuring electronic structure via W doped 1T MoS₂ for enhancing hydrogen evolution reaction. *Appl Sure Sci* 2022;579:152216.
4. Le K, Zhang X, Zhao Q, et al. Controllably doping nitrogen into 1T/2H MoS₂ heterostructure nanosheets for enhanced supercapacitive and electrocatalytic performance by low-power N₂ plasma. *ACS Appl Mater Inter* 2021;13:44427-39
5. Zhao X, Ma X, Lu Q, et al. FeS₂-doped MoS₂ nanoflower with the dominant 1T-MoS₂ phase as an excellent electrocatalyst for high-performance hydrogen evolution. *Electrochim. Acta* 2017;249:72-8.
6. Luo Z, Ouyang Y, Zhang H, et al. Chemically activating MoS₂ via spontaneous atomic palladium interfacial doping towards efficient hydrogen evolution. *Nat Commun* 2018;9:2120.

7. Lau TH, Wu S, Kato R, et al. Engineering monolayer 1T-MoS₂ into a bifunctional electrocatalyst via sonochemical doping of isolated transition metal atoms. *ACS Catalysis* 2019;9:7527-34.
8. Wang G, Zhang G, Ke X, et al. Direct synthesis of stable 1T-MoS₂ doped with Ni single atoms for water splitting in alkaline media. *Small* 2022;18:2107238.
9. Islam M, Nguyen TH, Tran DT, Dinh VA, Kim NH, Lee JH. Bimetallic atom dual-doped MoS₂-based heterostructures as a high-efficiency catalyst to boost solar-assisted alkaline seawater electrolysis. *ACS Sustainable Chem Eng* 2023;11:6688-97.
10. Wu W, Zhang X, Xiao Y, et al. Highly salt-tolerant hydrogen evolution reaction based on dendritic urchin-like MoC/MoS₂ heterojunction in seawater. *Chem Eng* 2024;480:148085.
11. Ma YY, Wu CX, Feng XJ, et al. Highly efficient hydrogen evolution from seawater by a low-cost and stable CoMoP@C electrocatalyst superior to Pt/C. *Energy Environ Sci* 2017;10:788-98.
12. Jin H, Liu X, Vasileff A, et al. Single-crystal nitrogen-rich two-dimensional Mo₅N₆ nanosheets for efficient and stable seawater splitting. *ACS Nano* 2018;12:12761-9.
13. Miao J, Lang Z, Zhang X, et al. Polyoxometalate-derived hexagonal molybdenum nitrides (MXenes) supported by boron, nitrogen codoped carbon nanotubes for efficient electrochemical hydrogen evolution from seawater. *Adv Funct Mater* 2019;29:1805893.
14. Chen IWP, Hsiao CH, Huang JY, Peng YH, Chang CY. Highly efficient hydrogen evolution from seawater by biofunctionalized exfoliated MoS₂ quantum dot aerogel electrocatalysts that is superior to Pt. *ACS Appl Mater Inter* 2019;11:14159-65.
15. Wu X, Zhou S, Wang Z, et al. Engineering multifunctional collaborative catalytic interface enabling efficient hydrogen evolution in all pH range and seawater. *Adv Energy Mater* 2019;9:1901333.
16. Huang W, Zhou D, Qi G, Liu X. Fe-doped MoS₂ nanosheets array for high-current-density seawater electrolysis. *Nanotechnology* 2021;32:415403.
17. Dang VD, Putikam R, Lin MC, Wei KH. MoS₂ nanoflowers grown on plasma-induced W-anchored graphene for efficient and stable H₂ production through seawater electrolysis. *Small* 2024;20:2305220.